Modeling lower critical solution temperature behavior of associating polymer brushes with classical density functional theory

Kai Gong, Bennett D. Marshall, and Walter G. Chapman

Citation: J. Chem. Phys. **139**, 094904 (2013); doi: 10.1063/1.4819957
View online: http://dx.doi.org/10.1063/1.4819957
View Table of Contents: http://jcp.aip.org/resource/1/JCPSA6/v139/i9
Published by the AIP Publishing LLC.

Modeling lower critical solution temperature behavior of associating polymer brushes with classical density functional theory

Kai Gong, Bennett D. Marshall, and Walter G. Chapman[a)]
Department of Chemical and Biomolecular Engineering, Rice University, 6100 S. Main, Houston, Texas 77005, USA

(Received 7 June 2013; accepted 20 August 2013; published online 6 September 2013)

We study the lower critical solution temperature (LCST) behavior of associating polymer brushes (i.e., poly(N-isopropylacrylamide)) using classical density functional theory. Without using any empirical or temperature-dependent parameters, we find the phase transition of polymer brushes from extended to collapsed structure with increasing temperature, indicating the LCST behavior of polymer brushes. The LCST behavior of associating polymer brushes is attributed to the interplay of hydrogen bonding interactions and Lennard-Jones attractions in the system. The effect of grafting density and molecular weight on the phase behavior of associating polymer brushes has been also investigated. We find no LCST behavior at low grafting density or molecular weight. Moreover, increasing grafting density decreases the LCST and swelling ratio of polymer brushes. Similarly, increasing molecular weight decreases the LCST but increases the swelling ratio. At very high grafting density, a partial collapsed structure appears near the LCST. Qualitatively consistent with experiments, our results provide insight into the molecular mechanism of LCST behavior of associating polymer brushes. © *2013 AIP Publishing LLC*. [http://dx.doi.org/10.1063/1.4819957]

I. INTRODUCTION

Temperature responsive polymers[1] such as poly(N-isopropylacrylamide) (PNIPAAM)[2] undergo a sharp conformation change near the lower critical solution temperature (LCST) of 32 °C. Below the LCST, the PNIPAAM chains are hydrophilic and expand in water. Above the LCST, the PNIPAAM chains become hydrophobic and collapse to avoid contact with water. A common method to exploit this feature is to graft PNIPAAM chains onto a surface.[3] This allows the surface properties to be controlled through temperature. Since the LCST (32 °C) is close to physiological temperature, PNIPAAM brushes have been utilized in various areas such as drug delivery,[4] protein adsorption,[5] cell adhesion,[6] and chromatography.[7]

To better tune conformation properties of PNIPAAM brushes for specific applications, it is very important to understand the PNIPAAM brushes phase behavior under different conditions such as molecular weight, grafting density, temperature, etc. It is noteworthy that the PNIPAAM brushes may act differently as compared to bulk aqueous solutions since they are constrained by one end to a surface. The dependence of PNIPAAM brush conformation change on different molecular weight and grafting density has been extensively investigated by using a number of experimental techniques including neutron reflectivity (NR),[8–11] atomic force microscopy (AFM),[12–15] quartz crystal microbalance measurements (QCM),[12,13,16,17] surface forces,[18–20] ellipsometry,[21] water contact angle measurement,[18,19] and surface plasmon resonance (SPR).[22] Generally, the molecular weight and grafting density are shown to be important for the phase behavior of PNIPAAM brushes. For example, Yim *et al.*[8–11] performed neutron reflectivity to obtain the monomer concentration profile of PNIPAAM brushes at a variety of molecular weight and grafting density. A distinct phase transition for the polymer brushes was found only at higher grafting density and molecular weight. In addition, a "bilayer" structure, which consists of a dense inner "phase" and a dilute outer "phase," was observed when the temperature is close to the LCST. They also found that the maximum change of polymer brush thickness with temperature was at intermediate grafting density and high molecular weight. Leckband *et al.*[18,19] conducted the surface force and water contact angle measurement for PNIPAAM brushes. In agreement with Yim *et al.*,[8–11] they found that the temperature-driven collapse transition for PNIPAAM brushes only happened at the higher grafting density and molecular weight. Bittrich *et al.*[21] used ellipsometry to measure the thickness of PNIPAAM brushes and observed similar behavior. They further demonstrated the decrease of hydrogen bonding interaction above the LCST by *in situ* attenuated total reflection Fourier-transform infrared (ATR-FTIR) spectroscopy measurements for PNIPAAM brushes. By using AFM and QCM-D, Ishida and Biggs[12,13] found that increasing grafting density decreased the LCST of PNIPAAM brushes.

While there are a large number of experimental works on PNIPAAM brushes, relatively few theoretical[23–28] and simulation[29] studies have been conducted to explain the LCST behavior of PNIPAAM brushes. Lee *et al.*[29] performed molecular dynamics simulation to investigate the deswelling mechanism of PNIPAAM brushes in water. They observed the deswelling of the PNIPAAM brushes above the LCST. They further found that it was mainly due to the decrease of the

a)Author to whom correspondence should be addressed. Electronic mail: wgchap@rice.edu. Tel.: (1) 713 348 4900. Fax: (1) 713 348 5478.

hydrogen bonding interaction between the amide groups and water molecules that caused the deswelling of PNIPAAM brushes with increasing temperature. Currently, most of the theoretical studies have been based on Flory-Huggins approach by using a phenomenological temperature-dependent χ parameter. Okada and Tanaka[30] explained the LCST behavior of PNIPAAM solutions by introducing the concept of cooperative hydration. Halperin *et al.*[23–26] generalized the mean-field theory of Pincus to describe the LCST behavior of PNIPAAM brushes by introducing an empirical χ parameter that depends on concentration and temperature. The model predicted a bilayer structure at the higher grafting density and a single layer profile at lower grafting density. Mendez *et al.*[27] used self-consistent field theory (SCFT) to study the effects of temperature, molecular weight, and grafting density on the equilibrium structure of PNIPAAM brushes. An empirical χ parameter obtained from the bulk phase diagram of PNIPAAM solutions was used as the input of their theory. They found that the maximum change of brush thickness was at intermediate grafting density and high molecular weight. The above theoretical studies provide some insight into the LCST behavior of PNIPAAM brushes.

It is well recognized that the LCST phase behavior of PNIPAAM results from a balance between hydrogen bonding interactions and the long range attraction. Without considering the hydrogen bonding interaction between the polymer and solvent, it is difficult to explain the sharp LCST behaviors. In this paper, the continuum space method based on Wertheim's theory[31–34] considers both the compressibility effect and hydrogen-bonding interaction and can provide molecular-level understanding to the nature of the LCST behavior. Jackson *et al.*[35–37] and Arndt and Sadowski[38] successfully used this type of method to study the LCST behavior of hydrogen bonding polymeric systems in the bulk. Bymaster and Chapman[39] developed the inhomogeneous statistical associating fluid theory (iSAFT) that incorporated the association interaction based on Wertheim's theory.[31–34] iSAFT has been successfully applied to study reentrant order-disorder phase transitions of associating polymeric systems. In this work, we used iSAFT to investigate the LCST behavior of associating polymer brushes. Rooted in statistical mechanics, density functional theory (DFT) has become a popular tool to model polymeric systems.[40–43] In comparison with simulation, DFT provides a more computationally efficient approach, especially when the solvent is explicitly included. McCoy *et al.*[44,45] and later Jain *et al.*[46] have extended DFT to polymer brush system. Their DFT results are in good agreement with simulation and follow the scaling relations proposed by Alexander[47] and de Gennes.[48] In our previous work, we successfully extended the work of Jain *et al.*[46] to study the phase behavior of mixed polymer brushes[49] and copolymer brushes.[50] In this paper, we extend the associating DFT of Bymaster and Chapman[39] to model the LCST behavior of associating polymer brushes. Also, we have studied the effect of molecular weight and grafting density on the LCST behavior. Our results are qualitatively consistent with experimental results. The paper is organized as follows: Sec. II explains the DFT model, Sec. III presents our results and corresponding discussion, and Sec. IV gives our conclusions.

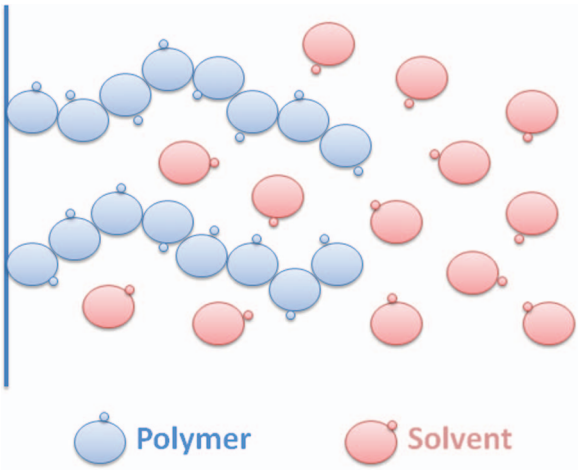

FIG. 1. Schematic illustration of associating polymer brushes immersed in explicit solvent.

II. THEORY

A. Interaction potential model

We consider associating polymer brushes (A) of chain length N_A in an explicit solvent (B). As shown in Figure 1, the polymer segment and solvent molecule have the same diameter σ. Each polymer segment has a single (type a) association site, and each solvent molecule has a single (type b) association site. These association sites represent hydrogen acceptor and hydrogen donor sites. The form of the association potential will be defined below. As an initial study, we assume heterogeneity only perpendicular to the surface, thus the possible lateral inhomogeneity in the associating polymer brushes have been neglected. The polymer brushes are modeled as freely jointed chains with one end tethered to a surface. The interaction potential between segments can be described as a sum of a hard sphere reference, a cut and shifted Lennard-Jones (LJ) attraction with a Weeks, Chandler, and Andersen (WCA) separation,[51,52] and association,

$$u(r_{12},\omega_1,\omega_2) = u^{hs}(r_{12}) + u^{att}(r_{12}) + \sum_a \sum_b u_{ab}^{assoc}(r_{12},\omega_1,\omega_2), \quad (1)$$

where r_{12} is the distance between two segments, ω_1 (ω_2) is the orientation of segment 1 (2), and

$$u^{hs}(r_{12}) = \begin{cases} \infty, & r_{12} < \sigma \\ 0, & r_{12} \geq \sigma. \end{cases} \quad (2)$$

The contribution due to long range attractions is

$$u^{att}(r_{12}) = \begin{cases} u^{LJ}(r_{min}) - u^{LJ}(r_c) & \text{if} \quad \sigma < r_{12} \leq r_{min} \\ u^{LJ}(r_{12}) - u^{LJ}(r_c) & \text{if} \quad r_{min} < r_{12} \leq r_c, \end{cases} \quad (3)$$

where

$$u^{LJ}(r_{12}) = 4\varepsilon^{LJ}\left[\left(\frac{\sigma}{r_{12}}\right)^{12} - \left(\frac{\sigma}{r_{12}}\right)^{6}\right], \quad (4)$$

$r_{min} = 2^{1/6}\sigma$ is the position of the Lennard-Jones potential minima, and $r_c = 3.5\sigma$ is the cutoff distance.

Finally, the association potential is given by

$$u_{ab}^{assoc}(r_{12},\omega_1,\omega_2)=\begin{cases}-\varepsilon_{ab}^{assoc}, & r_{12}<r_c;\theta_{a1}<\theta_C;\theta_{b2}<\theta_c\\ 0, & \text{otherwise},\end{cases} \tag{5}$$

where θ_{a1} is the angle between the vector from the center of segment 1 to site a and the vector r_{12} and θ_{b2} is the angle between the vector from the center of segment 2 to site b and the vector r_{12}. The radial limits of square-well association were set to $r_c = 1.05\sigma$ and the angular limit to $\theta_c = 27^\circ$. The surface is a smooth hard wall that is neutral (only repulsive) to the polymer brush segments and solvent molecules.

B. iSAFT density functional theory

The challenge in implementation of density functional theory is to construct the Helmholtz free energy functional. Based on thermodynamic perturbation theory, the total Helmholtz free energy functional can be decomposed into an ideal and excess contribution,

$$A[\rho_i(r)]=A^{id}[\rho_i(r)]+A^{ex,hs}[\rho_i(r)]+A^{ex,chain}[\rho_i(r)]+A^{ex,att}[\rho_i(r)]+A^{ex,assoc}[\rho_i(r)]. \tag{6}$$

The ideal contribution comes from the ideal gas state of the atomic mixture (id). The excess contribution of the free energy is due to excluded volume effects (hs), chain connectivity (chain), long-range attractions (att), and association (assoc).

The ideal gas functional is known exactly

$$\beta A^{id}[\rho_i(r)]=\int dr_1\sum_{i=1}^{N}\rho_i(r_1)[\ln\rho_i(r_1)-1]. \tag{7}$$

$A^{ex,hs}$ is calculated from Rosenfeld's fundamental measure theory (FMT)[53] for a mixture of hard spheres:

$$\beta A^{ex,hs}[\rho_i(r)]=\int dr\Phi[n_\alpha(r)], \tag{8}$$

where $\Phi[n_\alpha(r)]$ is given by

$$\Phi[n_\alpha(r)]=-n_0\ln(1-n_3)+\frac{n_1n_2-n_{v1}\cdot n_{v2}}{1-n_3}+\frac{n_2^3-3n_2n_{v2}\cdot n_{v2}}{24\pi(1-n_3)^2} \tag{9}$$

and n_α are the weighted densities (or fundamental measures).

For simplicity, the mean field approximation[54] is used for the attraction term:

$$\beta A^{ex,att}[\rho_i(r)]=\frac{1}{2}\sum_{i=1}^{N}\sum_{j=1}^{N}\int dr_1dr_2u_{ij}^{att}(|r_2-r_1|)\rho_i(r_1)\rho_j(r_2). \tag{10}$$

The mean-field approximation has been validated with simulation for several polymer systems.[46,55,56]

Wertheim's TPT1[31–34,57,58] is used to calculate $A^{ex,assoc}$ by forcing a mixture of spherical segments to bond in a specified order to form the polymer or solvent molecules of interest:

$$\beta A^{ex,assoc}[\rho_i(r)]=\int dr_1\sum_{i=1}^{N}\rho_i(r_1)\times\sum_{a\in\Gamma^{(i)}}\left(\ln\chi_a^i(r_1)-\frac{\chi_a^i(r_1)}{2}+\frac{1}{2}\right). \tag{11}$$

The first summation is over all segments i, and the second over all the association sites on segment i as $\Gamma^{(i)}$ is the set of all the associating sites on segment i. χ_a^i denotes the fraction of segments of type i that are not bonded at their associating site a, which can be obtained by the law of mass action,[57,58]

$$\chi_a^i(r_1)=\frac{1}{1+\int dr_2\chi_b^{i'}(r_2)\Delta^{ii'}(r_1,r_2)\rho_{i'}(r_2)}, \tag{12}$$

where i′ denotes the neighboring segment which bonds with segment i; site a on i bonds to site b on i′. For hard sphere segments that do not overlap,

$$\Delta^{ii'}(r_1,r_2)=KF^{ii'}(r_1,r_2)y^{ii'}(r_1,r_2), \tag{13}$$

where K is a constant geometric factor which accounts for the entropic cost associated with the orientations and bonding volume of two segments. $F^{ii'}(r_1,r_2)$ is the association Mayer-f function given as

$$F^{ii'}(r_1,r_2)=\left[\exp\left(\beta\varepsilon_0-\beta v_{bond}^{ii'}(r_1,r_2)\right)-1\right], \tag{14}$$

where ε_0 is the bond energy and $v_{bond}^{ii'}(r_1,r_2)$ is the bonding potential. In the complete association limit of $\varepsilon_0\to\infty$, the chain contribution to the free energy $A^{ex,chain}$ can be obtained. For tangentially bonded segments, the bonding potential is given by

$$\exp\left(-\beta v_{bond}^{ii'}(r_1,r_2)\right)=\frac{\delta(|r_1-r_2|-\sigma^{ii'})}{4\pi(\sigma^{ii'})^2} \tag{15}$$

and $y^{ii'}(r_1,r_2)$ is the cavity correlation function for the inhomogeneous hard sphere reference fluid.

We consider a system with fixed grafting density of the polymer brush (A) and fixed bulk chemical potential of the solvent (B), which is "semi-canonical" ensemble (V (volume), T (temperature), M_A (number of polymer segments), μ_B (chemical potential of solvent) are fixed). In this semi-canonical ensemble, the equilibrium density profile of polymer and solvent is obtained by minimizing the "semi-canonical free energy" functional

$$A'[\rho_i(r)]=A[\rho_i(r)]+\sum_i\int dr\rho_i(r)V_{ext}(r)-\int dr\rho_B(r)\mu_B. \tag{16}$$

(This semi-canonical free energy can be obtained by applying a Legendre transform from the Helmholtz free energy in the canonical ensemble.)

The constraint on the density of the polymer brush is given by

$$\int dr\rho_A(r)=M_A. \tag{17}$$

By using the Lagrange multiplier technique, we construct the free energy functional as

$$A[\rho_i(r)] + \sum_i \int dr \rho_i(r) V_{ext}(r) - \int dr \rho_B(r) \mu_B - \lambda_A \left[\int \rho_A(r) dr - M_A \right]. \quad (18)$$

By minimizing the above functional with respect to ρ_i, we can obtain

$$\frac{\partial A[\rho_i(r)]}{\partial \rho_A(r)} + V_{ext}(r) - \lambda_A = 0, \quad (19)$$

$$\frac{\partial A[\rho_i(r)]}{\partial \rho_B(r)} + V_{ext}(r) - \mu_B = 0. \quad (20)$$

As we can see, there are only three equations ((17), (19), and (20)) with three unknown variables ρ_A, ρ_B, and λ_A. To obtain the density profiles of each component, these three equations are solved simultaneously. The numerical algorithm is the same as in Jain *et al.*'s paper.[46] (λ_A is the chemical potential of the polymer brush in Jain *et al.*'s paper.[46,56] The association effect is added in Eqs. (6) and (11).) The above derivation is conducted to show that Jain *et al.*'s[46] DFT method of treating polymer brushes at fixed grafting density is an application of the semi-canonical ensemble. Thus, we compare this semi-canonical free energy A′ to determine the stable structure. The final expression for the semi-canonical free energy A′ is expressed as

$$\beta A'[\rho_i(r)] = \beta A^{ex,hs}[\rho_i(r)] + \beta A^{ex,att}[\rho_i(r)] + \beta A^{ex,assoc}[\rho_i(r)] + \int dr \sum_{i=1}^{N} \rho_i(r) \left[D_i(r) + \frac{n(\Gamma^{(i)})}{2} - 1 \right] + \int dr \rho_A(r) \lambda_A, \quad (21)$$

where $n(\Gamma^{(i)})$ is the total number of the bonding sites on segment i, and

$$D_i(r) = \frac{1}{2} \sum_{\gamma=1}^{N} \sum_{\gamma'}^{\{\gamma'\}} \int \rho_\gamma(r_1) \frac{\delta \ln y^{\gamma\gamma'}_{contact}[\{\bar{\rho}_i(r_1)\}]}{\delta \rho_i(r)} dr_1 - \frac{\delta \beta A^{ex,hs}}{\delta \rho_i(r)} - \frac{\delta \beta A^{ex,att}}{\delta \rho_i(r)} - \frac{\delta \beta A^{ex,assoc}}{\delta \rho_i(r)}, \quad (22)$$

where $y^{\gamma\gamma'}_{contact}[\{\bar{\rho}_i(r_1)\}]$ is the contact value of cavity correlation function at weighted density $\bar{\rho}_i(r_1)$. For the details of numerical procedure of solving the above equations, please refer to our previous work.[39,46]

III. RESULTS

In this section, we study the phase behavior of associating polymer brushes (A) in explicit monomer solvent (B). To minimize the large parameter space, we first fix the polymer brush length $N_A = 50$, grafting density $\rho_g \sigma^2 = 0.1$, and bulk solvent density $\rho_B \sigma^3 = 0.8$. The surface is located at $z = 0$. For simplicity, the interaction energy is set such that (1) the Lennard-Jones interaction energy $\varepsilon^{LJ}_{AA}/k_b = \varepsilon^{LJ}_{BB}/k_b = 218.4$ K, (2) hydrogen bonding (HB) interaction energy $\varepsilon^{assoc}_{AB}/k_b = 2730$ K, and (3) all other interactions are equal to 0. The parameters are chosen to mimic the balance between hydrogen bonding versus the van der Waals interactions of real systems. While simple, this model can still capture the essential physics of the associating polymer brush system.

Before discussing our results, we first define two useful parameters: the thickness of the polymer brush ⟨z⟩ and the swelling ratio (Sw) of the polymer brush. The thickness of the polymer brush ⟨z⟩ is defined as twice the first moment of the density profile $\rho(z)$,

$$\langle z \rangle = \frac{2 \int z \rho(z) dz}{\int \rho(z) dz}. \quad (23)$$

The swelling ratio of the polymer brush is defined as the brush thickness at desired temperature (T) divided by the one at T = 323 K,

$$Sw = \frac{\langle z \rangle_T}{\langle z \rangle_{323\,K}}. \quad (24)$$

Figures 2(a) and 2(b) show the density profiles (a) and not bonded fraction (b) of polymer brushes and solvent at T = 303 K. An advantage of our theory is that we can easily calculate the hydrogen-bonding fraction between the polymer brushes and solvent. At T = 303 K, the polymer brushes are well solvated. The whole domain can be divided into two regions: the polymer brush region, which contains both polymer segments and solvent, and the solvent region which contains pure solvent. For example, in Figure 2(a), the separation line is about z = 11. The solvents have a density of about 0.45 in the polymer brush region, which is almost the same concentration with the polymer segments. Their density profiles both have strong oscillation near the surface due to packing effects. In the polymer brush region, as we can see from Figure 2(b), about 70% of polymer segments are bonded with the solvent, while 90% of solvents are bonded with the polymer segments. In this case, the hydrogen bonding interaction between the polymer brushes and solvent dominates the system and the solvent can easily penetrate into polymer brush region. However, as the temperature is increased from 303 K to 307 K, the polymer brushes suddenly collapse and phase separation occurs, as shown in Figures 2(c) and 2(d). It is a very sharp transition, and the transition temperature is the LCST of the polymer brushes. The collapse of the polymer brushes is due to the LJ attraction which exists between polymer segments. As temperature is increased, the hydrogen bonding between the polymer brushes and solvents decreases, and the LJ attraction becomes the dominant factor that makes the polymer brushes collapse. Increasing loss of entropy that occurs with association with increasing temperature can overcome the energetic benefit of association. The treatment of the association in the theory is why this theory is able to describe the LCST behavior without empirical parameters. In particular, we notice that there is almost a "bilayer" of solvent that can penetrate into polymer brush region and stay close to the surface. This effect is entropic in nature, since the penetration cost of solvents is relatively small compared to the entropic cost due to the complete collapse of the polymer brushes. We expect that the penetration of solvent will become less with increasing the size of the solvent molecules. The effect of

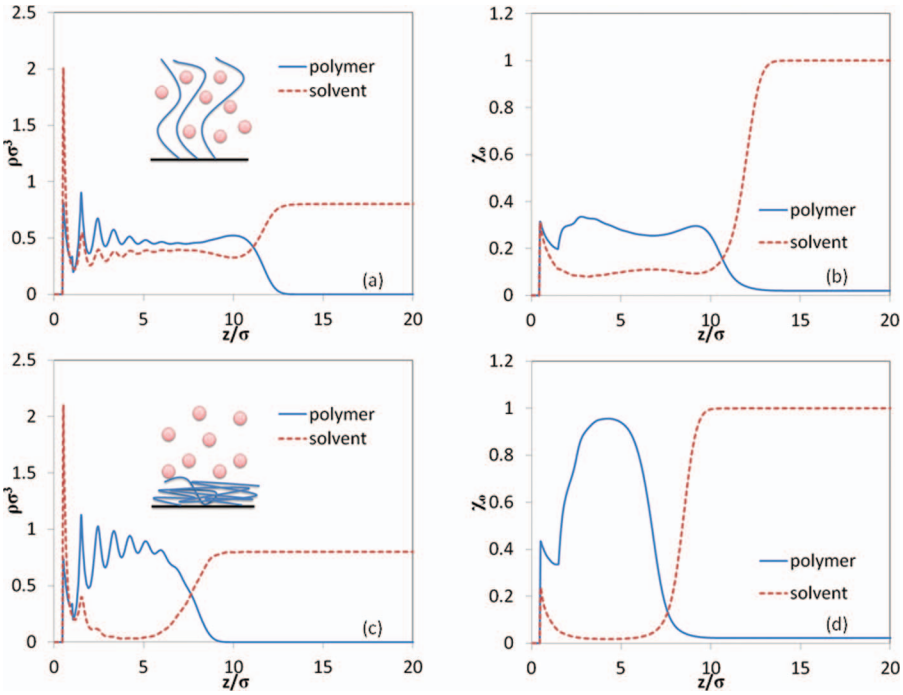

FIG. 2. (a) Density profiles of polymer brushes and solvent at T = 303 K. (b) Not bonded fraction of polymer brushes and solvent at T = 303 K. (c) Density profiles of polymer brushes and solvent at T = 307 K. (d) Not bonded fraction of polymer brushes and solvent at T = 307 K. Other parameters are fixed: the polymer brush length $N_A = 50$, grafting density $\rho_g\sigma^2 = 0.1$, and bulk solvent density $\rho_B\sigma^3 = 0.8$.

solvent properties will be considered in a future publication. Figure 2(d) shows that hydrogen bonds still form at the interface between the polymer brush and solvent. We also calculate the free energy for each state. The semi-canonical free energy versus T can be found in Figure 3. As shown in Figure 3, we can see the intersection (LCST = 305 K), which has a discontinuity of the slope, indicating the first order phase transition from the exposed to collapse structure with increasing temperature. Without using any empirical temperature-dependent parameter, our theory successfully captures the LCST behavior of hydrogen bonding polymer brushes.

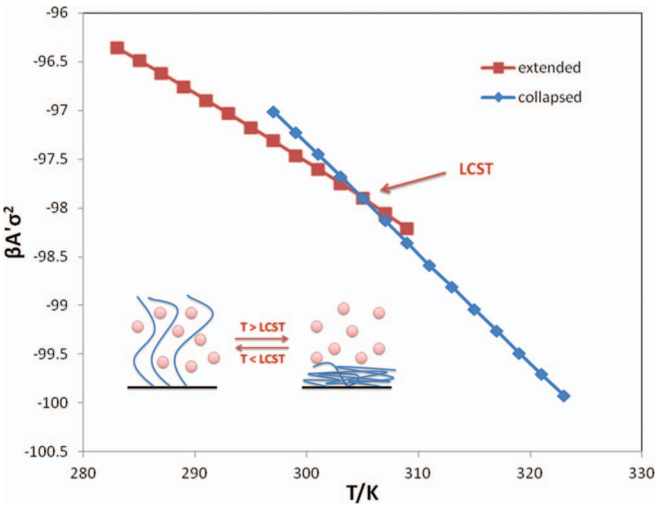

FIG. 3. Semi-canonical free energy (A′) versus temperature (T) (corresponding to Fig. 2). All the possible morphology (diamond (blue line): collapsed; rectangle (red line): extended) has been marked in the semi-canonical free energy diagram. The collapsed-extended structure phase transition happens at T = 305 K. The intersection between the collapsed-extended structure has a discontinuity of the slope, indicating the first-order phase transition.

As we increase the grafting density to a very high $\rho_g\sigma^2 = 0.2$, we find a partially collapsed structure (Figures 4(c) and 4(d)) in addition to the extended (Figures 4(a) and 4(b)) or the collapsed (Figures 4(e) and 4(f)) structure. This kind of structure has been observed in the Yim *et al.*'s experiments[11] and also predicted by Halperin *et al.*'s theoretical work with an empirical parameter χ.[23–26] In Figure 4(c), the partially collapsed structure is actually a mixing structure between the collapsed and the extended, since the inner part of the polymer brush is collapsed, while the outer part is well solvated. From Figure 4(d), the collapsed portion of the brush is depleted in solvent/polymer hydrogen bonds, while the outer extended portion of the brush exhibits a significant amount of hydrogen bonding. This partially collapsed structure is very stable at high grafting density and it only appears at the temperature close to the LCST. The appearance of the partially collapsed structure is involved with the entropic cost of folding polymer brush. At very high grafting density, the polymer brush cannot collapse completely due to the high entropic cost. This is different than the phase behavior of bulk polymer solutions. In Figure 5, from the semi-canonical free energy phase diagram, we can see the structure transits from extended to partial-collapsed to collapsed as the temperature is increased. Both transitions are first order since the slope of curves is different. (The curve for partial-collapsed structure does not connect to the collapsed state curve because partial-collapsed structure cannot be converged at higher temperature. This may be due to numerical instability of the current DFT methods.)

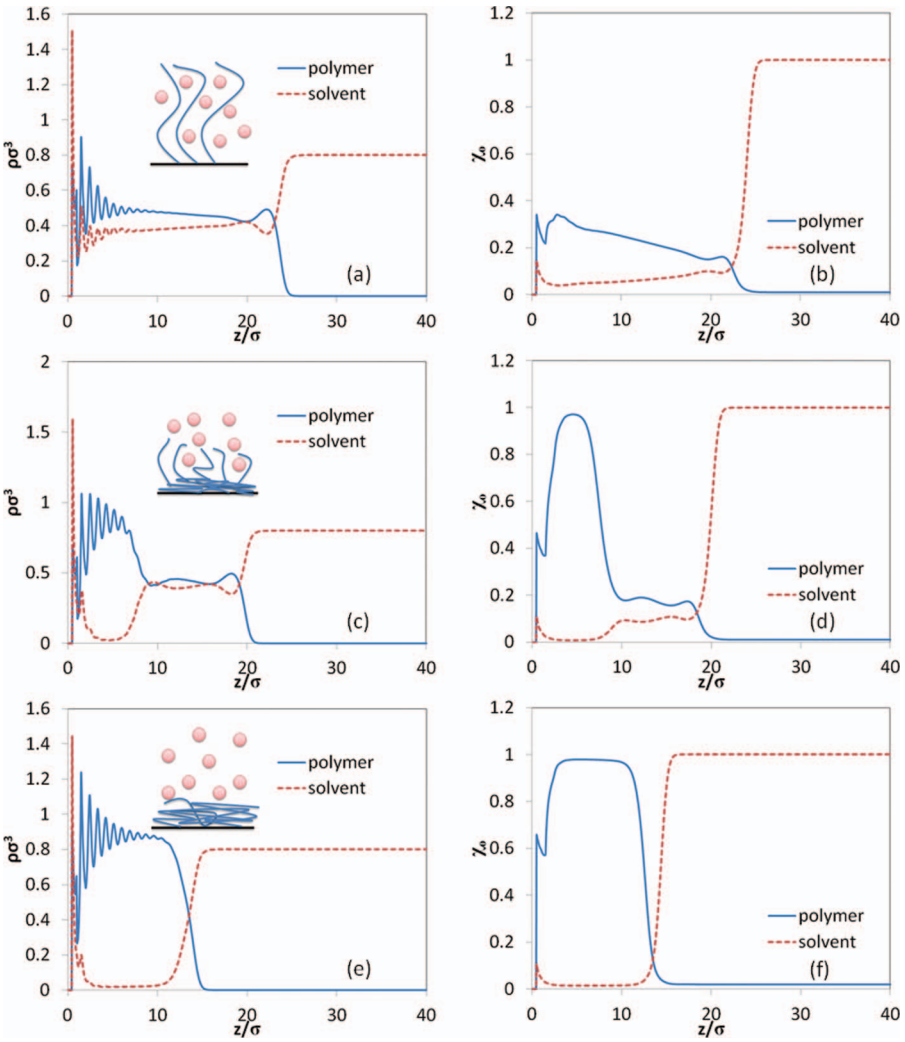

FIG. 4. (a) Density profiles of polymer brushes and solvent at T = 281 K. (b) Not bonded fraction of polymer brushes and solvent at T = 281 K. (c) Density profiles of polymer brushes and solvent at T = 285 K. (d) Not bonded fraction of polymer brushes and solvent at T = 285 K. (e) Density profiles of polymer brushes and solvent at T = 303 K. (f) Not bonded fraction of polymer brushes and solvent at T = 303 K. All the other parameters are the same with Fig. 2 except $\rho_g\sigma^2 = 0.2$.

The grafting density and molecular weight are considered as two important factors that affect the LCST behavior of polymer brushes. Since the swelling ratio of the polymer brush is very important for a specific application, we plot the swelling ratio of the polymer brush as a function of temperature in Figures 6 and 7. In Figure 6, the grafting density is varied from 0.05, 0.1, 0.15, and 0.2 to see its effect on the swelling ratio of polymer brush. At the lower grafting density $\rho_g\sigma^2 = 0.05$, there is no LCST behavior found for the polymer brushes, and its thickness shows a gradual decrease as temperature is increased. At $\rho_g\sigma^2 = 0.1$, we can see clearly a step change of swelling ratio at T = 305 K, indicating the phase transition or the LCST behavior of the polymer brush. The LCST behavior of the polymer brush is shown to happen only at higher grafting density, which is consistent with numerous experiments.[8–10,18,19,21] Increasing the grafting density from 0.1 to 0.15 decreases the LCST from 305 K to 297 K, the swelling ratio from about 1.6 to 1.4. The effect of grafting density on the LCST is qualitatively consistent with Ishida and Biggs's experiments.[12] The effect of grafting density on the swelling ratio is partially consistent with the viewpoint that intermediate grafting density and high molecular weight gives maximum swelling ratio change with temperature, which was shown by Mendez *et al.*'s SCFT results[27] and Yim *et al.*'s experiments.[8–10] At even higher grafting density $\rho_g\sigma^2 = 0.2$, due to appearance of partial-collapsed structure, the swelling ratio curve first has a discontinuity at 285 K (from extended to partial-collapsed), and then continuously decreases until a small step at 299 K (from partial-collapsed to extended).

The molecular weight (or the chain length) is another important parameter that can affect the phase behavior of the polymer brush. In Figure 7, we vary the chain length from 20, 50, 100, and 200 to see its effect on the swelling ratio of the polymer brush. At the lower chain length $N_A = 20$, no LCST behavior is found. Instead, a gradual decrease of brush thickness is observed with increasing temperature, similar to the previous lower grafting density case. The other three cases ($N_A = 50, 100, 200$) all show LCST behavior. Increasing the chain length from 50 to 100 leads to a decrease of LCST

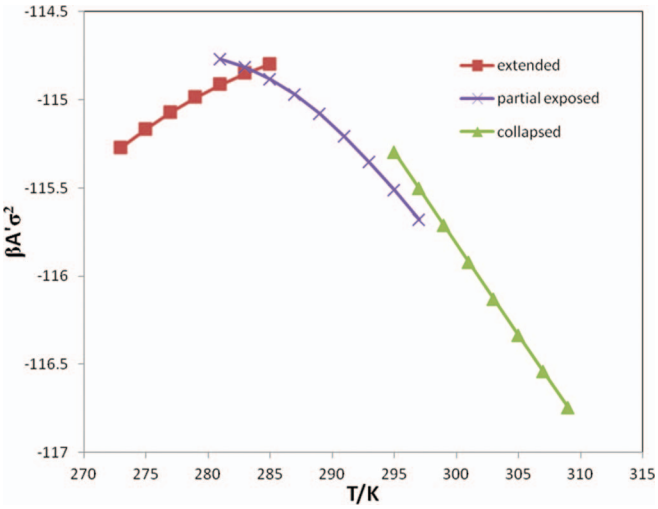

FIG. 5. Semi-canonical free energy (A′) versus temperature (T) at higher grafting density $\rho_g\sigma^2 = 0.2$ (corresponding to Fig. 4). All the possible morphology (triangle (green line): collapsed; cross (purple line): partial collapsed; rectangle (red line): extended) has been marked in the semi-canonical free energy diagram. The collapsed-partial collapsed structure phase transition happens at T = 299 K. The partial collapsed-extended structure phase transition happens at T = 285 K. The discontinuity of the slope for different structures indicates that both transitions are first order phase transition.

from 305 K to 297 K. However, we find the LCST changes little with an increase chain length from 100 to 200. In addition, the swelling ratio increases monotonically from about 1.6 to 1.9 with increasing N_A from 50 to 200, which is partially consistent with Mendez *et al.*'s SCFT results[27] and Yim *et al.*'s experiments.[8–10] The partially collapsed structure is not found at $N_A = 200$. However, it could reappear at even higher molecular weight.

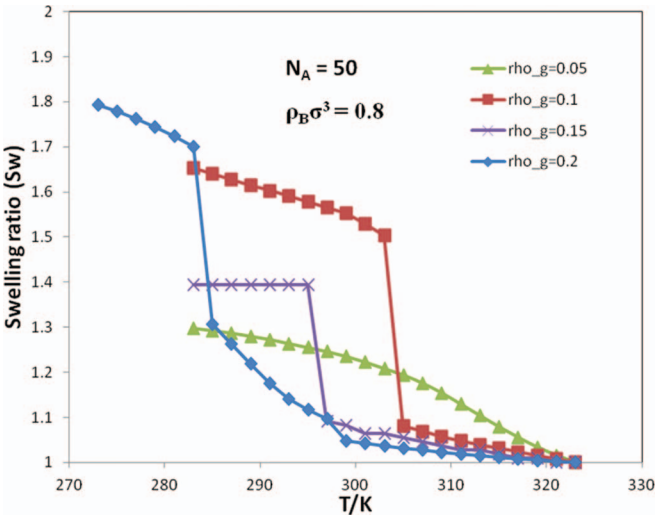

FIG. 6. Swelling ratio (Sw) of polymer brushes versus temperature (T) at different grafting densities: $\rho_g\sigma^2 = 0.05, 0.1, 0.15$, and 0.2. Other parameters are fixed: the polymer brush length $N_A = 50$ and bulk solvent density $\rho_B\sigma^3 = 0.8$.

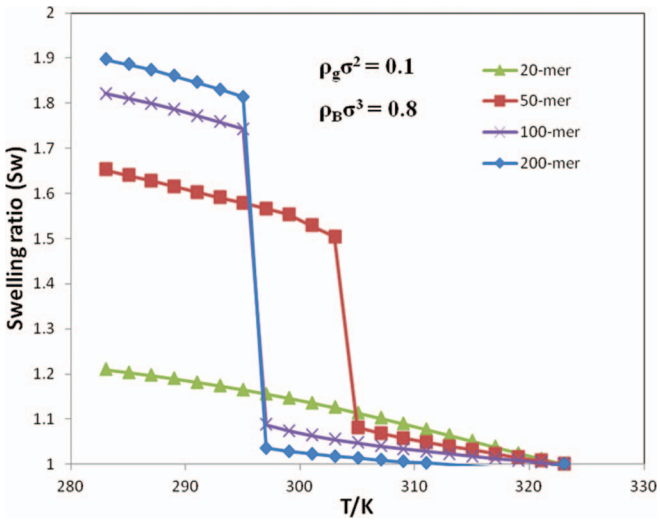

FIG. 7. Swelling ratio (Sw) of polymer brushes versus temperature (T) at different chain lengths: $N_A = 20$, 50, 100, and 200. Other parameters are fixed: grafting density $\rho_g\sigma^2 = 0.1$ and bulk solvent density $\rho_B\sigma^3 = 0.8$.

IV. CONCLUSIONS

Understanding the effect of molecular weight and grafting density on the LCST behavior of associating polymer brushes is of great importance for smart material design. In this work, we have employed a DFT to study systematically the large parameter space (i.e., molecular weight, grafting density, and temperature) that can affect the phase behavior of associating polymer brushes. Compared with molecular simulation, DFT has the great advantage of computational efficiency, especially when explicit solvent is included in the system. Consistent with experiments, our theory captures the LCST behavior of polymer brushes at higher grafting density and molecular weight. No LCST behavior is found at low molecular weight and grafting density. At very high grafting density, the partial collapsed structure is found near the LCST. Moreover, increasing grafting density decreases the LCST and swelling ratio of the polymer brush. Similarly, increasing molecular weight decreases the LCST but increases the swelling ratio of the polymer brush. This further demonstrates iSAFT's capability to capture the hydrogen bonding effect of the associating polymer systems.

ACKNOWLEDGMENTS

Financial support for this work was provided by the Robert A. Welch Foundation (Grant No. C-1241) and by the National Science Foundation (CBET-0756166).

We thank the reviewers for the constructive suggestions.

[1]M. A. C. Stuart, W. T. S. Huck, J. Genzer, M. Muller, C. Ober, M. Stamm, G. B. Sukhorukov, I. Szleifer, V. V. Tsukruk, M. Urban, F. Winnik, S. Zauscher, I. Luzinov, and S. Minko, Nature Mater. **9**(2), 101 (2010).
[2]H. G. Schild, Prog. Polym. Sci. **17**(2), 163 (1992).
[3]S. T. Milner, Science **251**(4996), 905 (1991).
[4]A. S. Hoffman, J. Controlled Release **6**(1), 297 (1987).
[5]D. L. Huber, R. P. Manginell, M. A. Samara, B.-I. Kim, and B. C. Bunker, Science **301**(5631), 352 (2003).
[6]Y. Akiyama, A. Kikuchi, M. Yamato, and T. Okano, Langmuir **20**(13), 5506 (2004).

[7]H. Kanazawa, K. Yamamoto, Y. Matsushima, N. Takai, A. Kikuchi, Y. Sakurai, and T. Okano, Anal. Chem. **68**(1), 100 (1996).
[8]H. Yim, M. S. Kent, D. L. Huber, S. Satija, J. Majewski, and G. S. Smith, Macromolecules **36**(14), 5244 (2003).
[9]H. Yim, M. S. Kent, S. Mendez, S. S. Balamurugan, S. Balamurugan, G. P. Lopez, and S. Satija, Macromolecules **37**(5), 1994 (2004).
[10]H. Yim, M. S. Kent, S. Mendez, G. P. Lopez, S. Satija, and Y. Seo, Macromolecules **39**(9), 3420 (2006).
[11]H. Yim, M. S. Kent, S. Satija, S. Mendez, S. S. Balamurugan, S. Balamurugan, and G. P. Lopez, Phys. Rev. E **72**(5), 051801 (2005).
[12]N. Ishida and S. Biggs, Macromolecules **43**(17), 7269 (2010).
[13]N. Ishida and S. Biggs, Langmuir **23**(22), 11083 (2007).
[14]N. Ishida and M. Kobayashi, J. Colloid Interface Sci. **297**(2), 513 (2006).
[15]D. M. Jones, J. R. Smith, W. T. S. Huck, and C. Alexander, Adv. Mater. **14**(16), 1130 (2002).
[16]G. Zhang, Macromolecules **37**(17), 6553 (2004).
[17]G. Liu and G. Zhang, J. Phys. Chem. B **109**(2), 743 (2005).
[18]K. N. Plunkett, X. Zhu, J. S. Moore, and D. E. Leckband, Langmuir **22**(9), 4259 (2006).
[19]X. Zhu, C. Yan, F. M. Winnik, and D. Leckband, Langmuir **23**(1), 162 (2007).
[20]I. B. Malham and L. Bureau, Langmuir **26**(7), 4762 (2010).
[21]E. Bittrich, S. Burkert, M. Müller, K.-J. Eichhorn, M. Stamm, and P. Uhlmann, Langmuir **28**(7), 3439 (2012).
[22]S. Balamurugan, S. Mendez, S. S. Balamurugan, M. J. O'Brie, and G. P. López, Langmuir **19**(7), 2545 (2003).
[23]A. Halperin, M. Tirrell, and T. P. Lodge, in *Macromolecules: Synthesis, Order and Advanced Properties* (Springer, Berlin, 1992), Vol. 100/1, p. 31.
[24]A. Halperin, Eur. Phys. J. B **3**(3), 359 (1998).
[25]V. A. Baulin and A. Halperin, Macromol. Theory Simul. **12**(8), 549 (2003).
[26]V. A. Baulin, E. B. Zhulina, and A. Halperin, J. Chem. Phys. **119**(20), 10977 (2003).
[27]S. Mendez, J. G. Curro, J. D. McCoy, and G. P. Lopez, Macromolecules **38**(1), 174 (2005).
[28]C.-L. Ren, R. J. Nap, and I. Szleifer, J. Phys. Chem. B **112**(50), 16238 (2008).
[29]S. G. Lee, T. A. Pascal, W. Koh, G. F. Brunello, W. A. Goddard, and S. S. Jang, J. Phys. Chem. C **116**(30), 15974 (2012).
[30]Y. Okada and F. Tanaka, Macromolecules **38**(10), 4465 (2005).
[31]M. S. Wertheim, J. Stat. Phys. **35**(1–2), 19 (1984).
[32]M. S. Wertheim, J. Stat. Phys. **35**(1–2), 35 (1984).
[33]M. S. Wertheim, J. Stat. Phys. **42**(3–4), 459 (1986).
[34]M. S. Wertheim, J. Stat. Phys. **42**(3–4), 477 (1986).
[35]P. Paricaud, A. Galindo, and G. Jackson, Mol. Phys. **101**(16), 2575 (2003).
[36]G. N. I. Clark, A. Galindo, G. Jackson, S. Rogers, and A. N. Burgess, Macromolecules **41**(17), 6582 (2008).
[37]M. N. García-Lisbona, A. Galindo, G. Jackson, and A. N. Burgess, J. Am. Chem. Soc. **120**(17), 4191 (1998).
[38]M. C. Arndt and G. Sadowski, Macromolecules **45**(16), 6686 (2012).
[39]A. Bymaster and W. G. Chapman, J. Phys. Chem. B **114**(38), 12298 (2010).
[40]J. Wu, AIChE J. **52**(3), 1169 (2006).
[41]C. P. Emborsky, Z. Feng, K. R. Cox, and W. G. Chapman, Fluid Phase Equilib. **306**(1), 15 (2011).
[42]Z. Feng, A. Bymaster, C. Emborsky, D. Ballal, B. Marshall, K. Gong, A. Garcia, K. Cox, and W. Chapman, J. Stat. Phys. **145**(2), 467 (2011).
[43]S. Tripathi and W. G. Chapman, Phys. Rev. Lett. **94**(8), 087801 (2005).
[44]J. D. McCoy, Y. Ye, and J. G. Curro, J. Chem. Phys. **117**(6), 2975 (2002).
[45]Y. Ye, J. D. McCoy, and J. G. Curro, J. Chem. Phys. **119**(1), 555 (2003).
[46]S. Jain, P. Jog, J. Weinhold, R. Srivastava, and W. G. Chapman, J. Chem. Phys. **128**(15), 154910 (2008).
[47]S. Alexander, J. Phys. (France) **38**(8), 983 (1977).
[48]P. G. de Gennes, *Scaling Concepts in Polymer Physics* (Cornell University, Ithaca, NY, 1979).
[49]K. Gong and W. G. Chapman, J. Chem. Phys. **135**(21), 214901 (2011).
[50]K. Gong, B. D. Marshall, and W. G. Chapman, J. Chem. Phys. **137**(15), 154904 (2012).
[51]D. Chandler and J. D. Weeks, Phys. Rev. Lett. **25**(3), 149 (1970).
[52]J. D. Weeks, D. Chandler, and H. C. Andersen, J. Chem. Phys. **54**, 5237 (1971).
[53]Y. Rosenfeld, Phys. Rev. Lett. **63**(9), 980 (1989).
[54]J. P. Hansen and I. R. McDonald, *Theory of Simple Liquids* (Academic, San Diego, CA, 1986).
[55]D. Cao and J. Wu, Macromolecules **38**(3), 971 (2005).
[56]S. Jain, A. Dominik, and W. G. Chapman, J. Chem. Phys. **127**(24), 244904 (2007).
[57]B. C. J. Segura, W. G. C. Shukla, and P. Keshawa, Mol. Phys. **90**(5), 759 (1997).
[58]W. G. Chapman, Ph.D. dissertation, Cornell University, 1988.